

Vibration isolation from irregularity in a nearly periodic structure: Theory and measurements

C. H. Hodges and J. Woodhouse

Topexpress Ltd., 1 Portugal Place, Cambridge CB5 8AF, England

(Received 22 December 1982; accepted for publication 25 May 1983)

This article describes the theory and a simple experiment carried out to demonstrate the phenomenon of Anderson localization in an acoustical context. This is an effect whereby the propagation of vibration in a structure which is not entirely regular is impeded by the irregularities, giving rise on the average to an exponential decay of vibration level away from the driving point, even in the absence of any dissipation. The structure used in the experiment was a stretched string with masses attached to it. This string was studied with regular spacings of the masses and after the masses had been moved in a controlled way to provide a small degree of irregularity. In both cases, the transmission of energy from end to end of the string was measured as a function of frequency, and also the mode shapes in the second and fourth passbands were measured so as to demonstrate the underlying physics of the localization phenomenon, in which the individual modes making up each passband change from being extended throughout the structure in the regular case to being localized in specific areas of the structure in the presence of irregularity. All measurements yielded satisfactory agreement with the theoretical predictions.

PACS numbers: 43.40.Cw, 43.40.Tm, 43.40.At

INTRODUCTION

A recent article¹ has described in acoustical terms the phenomenon of Anderson localization in disordered systems. This is an effect much studied in the field of solid state physics, but which is not widely recognized in acoustics (although there is some recent acoustical work touching on this subject²⁻⁴). This article describes further theory of the phenomenon, and a series of experiments carried out on the simplest structure which we could find to illustrate the localization effect in action and to test quantitative theoretical predictions. The structure used was a stretched string with a number of essentially identical masses attached to it. First, the masses were positioned, as nearly as possible, regularly along the string, then at a later stage the measurements were repeated with the masses displaced slightly from these regularly spaced positions to introduce a small amount of disorder. The experiments confirm the theory to a satisfactory degree, and the measurements provide a simple concrete illustration of the localization effect in action and also an easily grasped application of the general theory.

We first give a brief qualitative account of the localization effect, in a form which will apply to the experiment to be described below. Consider a row of N identical pendula, each one weakly coupled to its two neighbors with all couplings identical. This constitutes the simplest model of a one-dimensional periodic system, and if we imagine driving this chain at one end and observing at the other end, we will find the well-known behavior of pass and stop bands. For frequencies within the passband, vibrations can propagate unattenuated along the chain. For frequencies outside this range, that is within the stop bands, vibration cannot propagate along the chain at all: an exponentially decaying near-field around the driving point is generated.

We now need to understand this effect of pass and stop bands in terms of the vibration modes of the chain. If the couplings between the pendula were removed completely, it is obvious that the vibration modes of the N independent pendula would consist simply of each pendulum separately, vibrating at its natural frequency. Since the pendula are identical, these frequencies are all the same. Thus in this limit where the coupling has gone to zero, we have an N -fold degeneracy of mode frequencies. Now when we allow non-vanishing but small coupling, this degeneracy will be split, producing a cluster of frequencies all close to the resonance frequency of the uncoupled pendula. This cluster of frequencies is the passband.

The vibration modes associated with the frequencies in this band are well known,⁵ each mode having a vibration amplitude which varies sinusoidally with distance along the chain. The important point is that all the modes are *extended* throughout the whole structure. This is necessary to explain the phenomenon of unattenuated transmission in the passband. We can see this by writing the transfer admittance $Y(x, x'; \omega)$ from one point x to another x' on the chain in the usual form as a sum over modes:

$$Y(x, x'; \omega) = \sum_r \frac{i\omega w_r(x)w_r(x')}{\Omega_r^2 + 2i\omega\Delta_r - \omega^2}, \quad (1)$$

where $w_r(x)$ is the r th mode, with vibration frequency Ω_r , and damping factor Δ_r . It is clear that the transmission from x to x' is governed by the product of mode amplitudes at those two points for each mode in the sum. Thus for this transmission to be strong within the passband for any pair of points x and x' , the individual modes must indeed be extended throughout the structure.

If we now allow some disorder in the system by making

the pendula have slightly different natural frequencies, the character of the mode shapes changes. It is intuitively clear that, at least if the pendulum frequencies are sufficiently different, the modes will now be *localized* around individual pendula. Since the individual pendulum frequencies are no longer degenerate, the coupling between pendula is no longer strong enough to produce extended modes in which all pendula contribute more or less equivalent amplitudes.

Thus when we consider transmission from one point to another along the disordered chain of pendula, we see that the effect of disorder is to reduce that transmission. The mode amplitudes at two well-separated points will now be such that their product is always small, since a mode which is strong at one point will decay away from there, and will thus have only small amplitude at the distant point. This is the basic phenomenon which we seek to illustrate by the experiments described below: transmission between distant points on such a chain is less in the disordered case than in the regular case, and this is caused by a change of character of the vibration modes from extended to localized. Localization was first studied by P. W. Anderson,⁶ and is therefore known as Anderson localization. (The work of Anderson and Mott on localization and its applications to solid-state physics was cited in their Nobel prize of 1977.⁷)

The model of coupled pendula which we have just described seems very idealized, but we shall show in the next section that in fact it is relevant to the experiment which we have carried out on a stretched string with attached masses. Since the detailed theory of the pendulum model was not discussed in the previous article, in Sec. II we derive the results for that model which we shall need to interpret the experimental measurements. The experiments are described in detail in Sec. III, and a quantitative comparison of the results with the theoretical predictions from Secs. I and II is given in Sec. IV. This comparison shows very satisfactory agreement between theory and experiment, and therefore gives a strong indication that the phenomenon of Anderson localization can be very important in structural vibration and deserves further study in that context.

I. THE PENDULUM MODEL

It is first necessary to consider in more detail the behavior of the system of coupled pendula described above. Consider a chain of pendula as sketched in Fig. 1, with the k th pendulum having a natural frequency ω_k , and each pendulum coupled to its neighbors by a spring of strength V . If c_k is the displacement of the k th pendulum, the equation of mo-

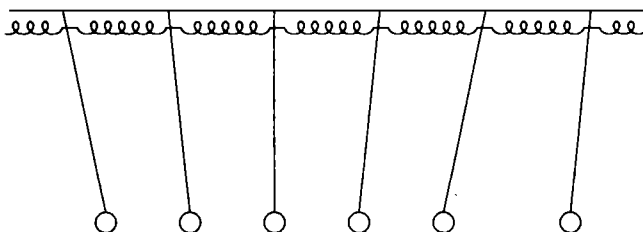


FIG. 1. Sketch of part of a chain of pendula coupled by springs.

tion for the k th pendulum in the chain at frequency ω is

$$Vc_{k+1} + U_k c_k + Vc_{k-1} = 0, \quad (2)$$

where

$$U_k = \omega^2 - \omega_k^2 - 2V. \quad (3)$$

For the case of identical pendula, with all ω_k equal to Ω say, it is well known⁵ that the normal modes on an infinite chain have the form

$$c_k = e^{ikq}, \quad (4)$$

where q ranges from 0 to π to specify the different modes. Substituting into Eq. (2) gives

$$\omega^2 = \Omega^2 + 2V(1 - \cos q), \quad (5)$$

so we see that all the modal squared frequencies lie in the range $\Omega^2 < \omega^2 < \Omega^2 + 4V$, which is therefore the passband for this periodic chain of pendula. Note that Eq. (5) relates the width of the passband to the coupling strength V ; this will prove useful in interpreting the experiments, where we can use the width of passbands (which are directly observable) to infer strengths of the equivalent coupling springs.

We now show that the pendulum model is relevant to our experiment, which used a stretched string with attached masses. We do this by a simple procedure based on Rayleigh's principle, for the appropriate regime of weak coupling of the sections of string via the masses. For brevity, we shall refer to the sections of the string between the masses as "bays." Let the length of the k th bay be $1 + \epsilon_k$, with $|\epsilon_k| \ll 1$ for all k . We suppose all the masses to be equal, with mass m . This mass is assumed much greater than the mass of string in a typical bay, for simplicity. This amounts to an assumption of weak coupling between the bays.

If the masses were infinite, each bay on the string would have its n th resonance at the same frequency, when the string in the bay vibrates with a sinusoidal mode shape having n half-cycles between the ends. We aim to understand the passbands resulting from the coupling through the masses of these resonances of each bay. We thus introduce suitable generalized coordinates to describe this motion of the bays as well as small motions of the masses, express the potential and kinetic energies of the system in terms of these coordinates, and minimize the Rayleigh quotient to obtain approximations to the coupled modes and their frequencies.

We suppose the amplitude of motion of the k th mass is b_k , and the amplitude of sinusoidal motion in the k th bay a_k . Consistent with our assumption of weak coupling between the bays, we suppose that the additional motion of the string resulting from motion of the masses simply forms a straight line between the masses. Thus we have the total motion of the string in the k th bay

$$y_k(x) = a_k \sin \frac{n\pi x}{1 + \epsilon_k} + b_{k-1} + (b_k - b_{k-1}) \frac{x}{1 + \epsilon_k}. \quad (6)$$

Now the potential energy P is given by

$$P = \frac{t}{2} \sum_{\text{bays}} \int_0^{1 + \epsilon_n} y'_k(x)^2 dx \simeq \frac{n^2 \pi^2 t}{4} \sum_{\text{bays}} \frac{a_k^2}{1 + \epsilon_k}, \quad (7)$$

when $|b_k| \ll |a_j|$ for all k and j , where t is the tension in the string. Similarly, when the angular frequency of oscillation is

ω , the kinetic energy is $\omega^2 T$ where

$$T = \frac{\rho}{2} \sum_{\text{bays}} \int_0^{1+\epsilon_n} y_k(x)^2 dx + \frac{m}{2} \sum_{\text{masses}} b_k^2 \quad (8)$$

$$\begin{aligned} &\simeq \frac{\rho}{2} \sum_{\text{bays}} (1 + \epsilon_k) \left(\frac{a_k^2}{2} + \frac{2a_k [b_{k-1} - (-1)^n b_k]}{n\pi} \right) \\ &+ \frac{m}{2} \sum_{\text{masses}} b_k^2, \end{aligned} \quad (9)$$

when $|b_k| \ll |a_j|$ for all k and j , where ρ is the line density of the string and $m \gg \rho$.

Now we take partial derivatives of $(P - \omega^2 T)$ with respect to a_k and b_k in turn, and equate both to zero to obtain

$$\frac{n^2 \pi^2 t a_k}{2(1 + \epsilon_k)} - \rho \omega^2 (1 + \epsilon_k) \left(\frac{a_k}{2} + \frac{[b_{k-1} - (-1)^n b_k]}{n\pi} \right) \simeq 0 \quad (10)$$

and

$$(\rho/n\pi) [a_{k+1}(1 + \epsilon_{k+1}) - (-1)^n a_k(1 + \epsilon_k)] + m b_k \simeq 0. \quad (11)$$

Let us identify

$$\begin{aligned} \omega_k^2 &\equiv \frac{n^2 \pi^2 t}{\rho(1 + \epsilon_k)^2}, \quad V \equiv \frac{2\rho\omega^2}{n^2 \pi^2 m}, \\ c_k &\equiv (-1)^{nk} a_k(1 + \epsilon_k), \end{aligned} \quad (12)$$

so that

$$\frac{(\omega^2 - \omega_k^2)}{(1 + \epsilon_k)} c_k \simeq V(2c_k - c_{k-1} - c_{k+1}). \quad (13)$$

Apart from the factor in the denominator on the left-hand side this is now in precisely the form of Eq. (2) for a chain of coupled pendula, with slightly differing pendulum frequencies. The variation in the coefficient of c_k is in fact dominated by that of $\omega^2 - \omega_k^2$ and to a good approximation the variation of denominator may be neglected. The coupled modes and their squared frequencies are now the eigenvectors and eigenvalues of a tridiagonal matrix with all off-diagonal terms equal (representing the coupling between pendula) and with the diagonal terms slightly disordered (representing mainly the squared frequencies of the uncoupled pendula). Thus the pendulum model is indeed relevant to our experiment.

One particular consequence of the above analysis is that in the periodic case the vibration modes in any single passband should look like those of eight coupled pendula. The actual shapes of the string in those modes for the second passband are illustrated in Fig. 2(a). In Fig. 2(b) are shown the mode shapes for the first passband, not dealt with explicitly above because of the approximation made, in which the string vibrates at rather low frequencies with the sections of the string between each pair of masses essentially straight. These modes are the standard textbook "masses on a mass-

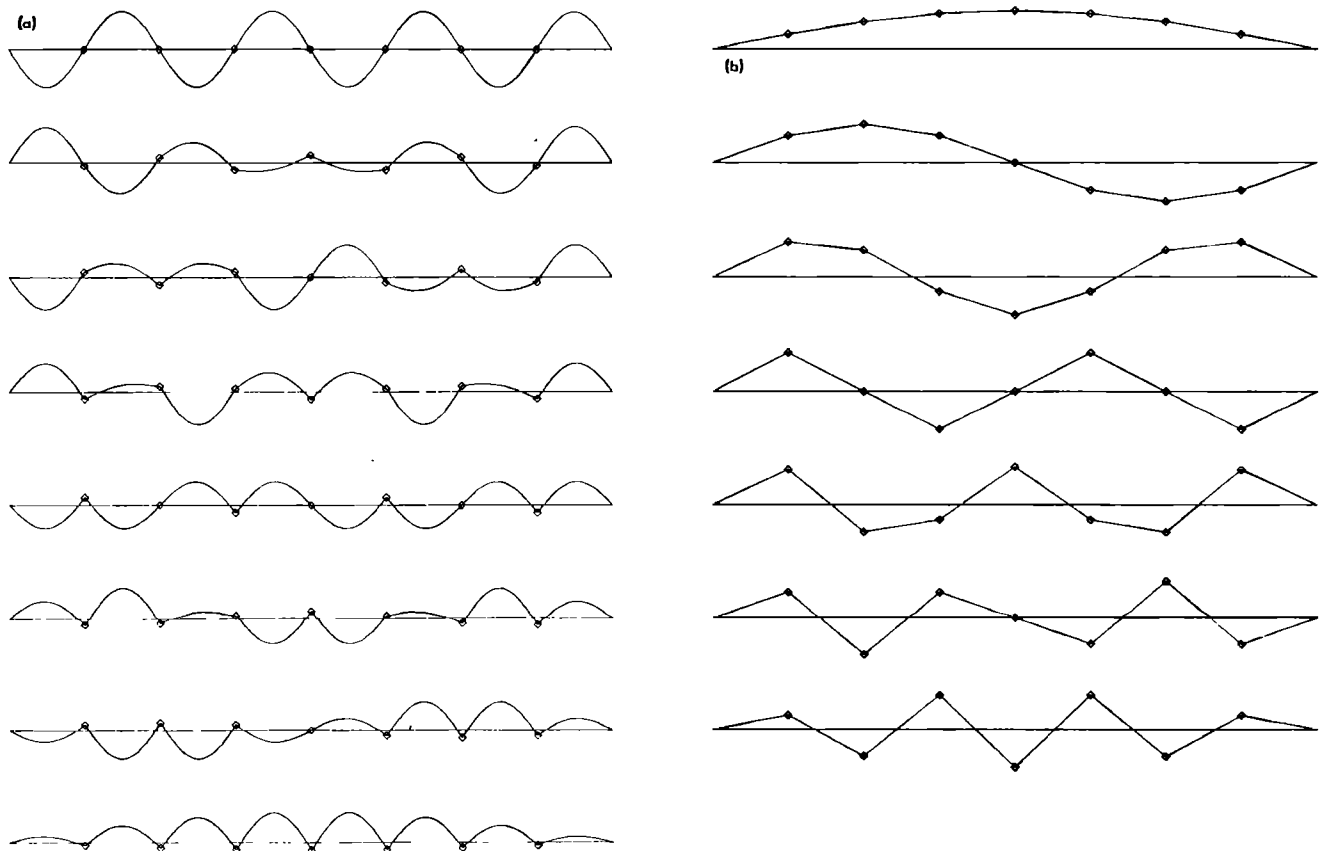


FIG. 2. (a) Mode shapes in the second passband of a string with seven equally spaced point masses attached. The lowest frequency is at the top. (b) Mode shapes in the first passband of a string with seven equally spaced point masses attached. The lowest frequency is at the top.

less string" modes used widely to illustrate Lagrange's equations (e.g., Rayleigh,⁸ §120).

One feature of Fig. 2(a) may seem contrary to immediate intuition. On the basis of a bogus use of Rayleigh's principle, one might have expected the mode in which the masses do not move to have a higher frequency than the other modes in the band, in all of which the masses do move. In fact, it has the lowest frequency. We can however give a genuine argument based on Rayleigh's principle which explains why the frequencies are in this apparently reversed order within the band. Consider first what happens if the masses are allowed to tend to infinity. In that case, the coupling between bays on the string tends to zero, and the width of the band shrinks to a single frequency. As the masses are made smaller than this, it is clear that the mode in which the masses do not move is uninfluenced, so it stays at that original single frequency. All the other modes must however move higher in frequency, from the general theorem that decreasing masses in any system without changing stiffnesses makes all frequencies move upwards, except for motions in which the masses do not move (Ref. 8, §88). Thus with our finite but relatively large masses, the modes must appear in the band in the order shown in Fig. 2(a).

II. LOCALIZATION IN THE PENDULUM MODEL

Having seen that the pendulum model is appropriate to our experiment we now investigate the localization behavior of that model to obtain predictions with which to compare the measurements. The theory presented previously¹ is appropriate to the case where variations in mass spacing are large compared to the wavelength on the string. Here we are concerned with variations in spacing which are small and of the order of 2% of the wavelength (see below). We proceed by outlining a general approach to the one-dimensional pendulum model with disorder, due originally to Herbert and Jones⁹ and subsequently elaborated by Thouless.¹⁰ The theory proceeds most simply for a finite chain of N pendula which is driven at one end and whose response is measured at the other. This is in fact the case appropriate to the experiments described in this paper but it will be argued later that the results are also relevant to the case where the chain is driven and measured at interior points. In the present case Eq. (2) is complemented by

$$V c_2 + U_1 c_1 = F$$

and

$$U_N c_N + V c_{N-1} = 0 \tag{14}$$

for the end pendula. Thus pendulum 1 is driven by a force $F e^{i\omega t}$ and we wish to determine the response x_N at the other end.

We shall assume that the pendulum natural frequencies are randomly distributed about a mean Ω , say, with some statistical distribution. It is simplest to assume ω_k^2 to lie with uniform probability in the interval $\Omega^2 - W$ to $\Omega^2 + W$ where W is a measure of the disorder. By dividing through Eq. (2) by V one can see that the mode shapes and hence the degree of localization depend only on the dimensionless disorder-to-coupling ratio W/V .

Solving the simultaneous Eqs. (2) and (14) is equivalent to inverting the matrix $\omega^2 I - M$ given by

$$\omega^2 I - M = \begin{bmatrix} U_1 & V & 0 & \dots & \dots & \dots & 0 \\ V & U_2 & V & \dots & \dots & \dots & 0 \\ 0 & V & U_3 & \dots & \dots & \dots & 0 \\ \dots & \dots & \dots & \dots & \dots & \dots & \dots \\ \dots & \dots & \dots & \dots & \dots & \dots & \dots \\ \dots & \dots & \dots & \dots & U_{N-1} & V & \dots \\ 0 & 0 & 0 & \dots & \dots & V & U_N \end{bmatrix}, \tag{15}$$

where I is the unit matrix. Thus in particular

$$x_N = R_{1N} F,$$

where $R = (\omega^2 I - M)^{-1}$. A matrix of the form in Eq. (15), with nonzero elements restricted to three diagonals, is called tridiagonal. Herbert and Jones noticed that the inverse element R_{1N} of such a matrix is easy to determine by the standard method of cofactors—the relevant minor determinant is readily seen to have the particularly simple form V^{N-1} . Therefore

$$R_{1N} = (-V)^{N-1} / \det(\omega^2 I - M). \tag{16}$$

This is a useful form of the result because there exist expansion procedures for the logarithm of the determinant in Eq. (16), both in the weak coupling-to-disorder and weak disorder-to-coupling limits.

Motivated by the solid-state work on Anderson localization, and also by our previous work applying this theory to acoustics,¹ we expect to find that for a typical disordered system within our ensemble the response decays exponentially on average away from the driving point. Thus we choose to analyze our present model by expressing the response as the exponential of a (complex) constant times the distance from the driving point. From Eq. (16) one may write the exponential decay constant for the response as the real part of

$$\gamma = -N^{-1} \ln R_{1N} = N^{-1} \ln [\det(\omega^2 I - M)] - \ln V. \tag{17}$$

An important property of this expression is that it tends to a limit as N , the length of the chain, goes to infinity. This can be seen by transforming to normal mode coordinates where M is diagonal. Disregarding any implicit frequency dependence of M one obtains

$$\gamma = -\ln V + N^{-1} \sum_r \ln(\omega^2 - \Omega_r^2), \tag{18}$$

where Ω_r are the normal mode frequencies. This in turn can be expressed in terms of the spectral density of modes $\rho_m(\omega)$ as

$$\gamma = -\ln V + N^{-1} \int d\omega' \rho_m(\omega') \ln(\omega^2 - \omega'^2). \tag{19}$$

Note that the smoothed modal density can be used here since the integral is well behaved as ω tends to ω' . Now it is a well-known result that the modal density of a spatially homogeneous system is proportional to its size (see for example Chap. VI, §4 of Courant and Hilbert¹¹). It is plausible, and general-

ly accepted,¹² that the same is true for a large homogeneously disordered system, apart from random fluctuations. In our case the mode density is thus proportional to N with fluctuations of order \sqrt{N} . Therefore as the length of the chain goes to infinity factors of N cancel out in the equation of γ . One is forced to conclude that if the response decays, it must eventually fall off exponentially with N . For the two limiting cases which we can treat in detail, we shall now demonstrate explicitly that this plausibility argument is indeed correct.

We wish to develop γ in a perturbative expansion, writing

$$M = M_0 + M_p$$

and expanding in powers of the perturbation M_p . For the case of weak coupling-to-disorder ($V/W \ll 1$) we take M_0 to be the diagonal part of M , representing uncoupled pendula, and M_p to be the off-diagonal coupling matrix. For the case of weak disorder-to-coupling ($W/V \ll 1$) we choose M_0 to be the full matrix M excluding the disorder, i.e., with $U_k = \omega^2 - \Omega^2 - 2V$, and M_p to be a diagonal matrix containing the deviations from the mean of the pendulum squared frequencies.

The matrix manipulations required to expand the logarithm of the determinant in Eq. (17) are not entirely straightforward and are discussed in the Appendix. One obtains the expansion

$$\gamma = -\ln V + N^{-1} \text{tr} \{ \ln(R_0) - R_0 M_p - \frac{1}{2} R_0 M_p R_0 M_p - \dots \}, \quad (20)$$

where

$$R_0 = (\omega^2 I - M_0)^{-1}.$$

In Eq. (20) tr denotes the trace of the matrix in curly brackets. We can now use this to discuss the two cases of weak coupling and weak disorder mentioned above.

A. Weak coupling $V/W \ll 1$

In this case we have

$$(M_0)_{kj} = (\omega^2 - U_k) \delta_{kj}$$

and

$$(M_p)_{kj} = V_{kj},$$

where the coupling matrix $V_{kj} = V$ for $k - j = \pm 1$ and zero otherwise. Equation (20) written out in suffix form then becomes

$$\gamma = N^{-1} \sum_k \ln(U_k) - \ln V - N^{-1} \sum_k \left(\frac{1}{2} \sum_j u_k V_{kj} u_j V_{jk} + \dots \right), \quad (21)$$

with $u_k = U_k^{-1}$. [Note that the term $R_0 M_p$ in Eq. (20) has zero trace in this case.]

We are concerned to estimate the decay constant of a typical disordered chain of pendula drawn from our statistical population, for which the natural frequencies ω_k vary randomly along the chain according to some statistical law. We shall not discuss here the separate and rather tricky problem of ensemble averaging, which was alluded to in the previous article¹ and which we intend to take up on a later

occasion. For typical long chains the sums over k in Eq. (21) may be estimated from the statistics. Thus in particular when U_k is uniformly distributed between $\omega^2 - \Omega^2 - 2V \pm W$, the typical value of the amplitude decay constant α is given by

$$\alpha = \text{Re } \gamma = \ln(W/V) - 1 + O(V^2/W^2) \quad (22)$$

at midband ($\omega^2 = \Omega^2 + 2V$).

B. Weak disorder, $W/V \ll 1$

For this case M_0 is the complete matrix M excluding the disorder so that M_0 represents the ordered chain with coupling and with all ω_k equal to Ω . The perturbation M_p is diagonal and fluctuates from pendulum to pendulum:

$$(M_p)_{kj} = (\omega_k^2 - \Omega^2) \delta_{kj} \equiv K_k \delta_{kj}. \quad (23)$$

In this case the two logarithmic terms in Eq. (20) must give the decay constant γ_0 for the ordered chain. This can be verified by substitution of the modal density of an infinite, periodic chain in Eq. (19); evaluation of the integral then reproduces the well-known behavior of periodic systems—in particular $\text{Re } \gamma_0$ is zero in the passbands of an infinite chain.

Written out in suffix notation, Eq. (20) now becomes

$$\gamma = \gamma_0 - N^{-1} \sum_k \left((R_0)_{kk} K_k + \frac{1}{2} \sum_j (R_0)_{kj} K_j (R_0)_{jk} K_k + \dots \right). \quad (24)$$

In this equation one may use outgoing boundary conditions for the matrix R_0 which then has the particularly simple form:

$$(R_0)_{kj} = -i(2V \sin q)^{-1} \exp(iq|k - j|) \quad (25)$$

with the propagation constant q defined by Eq. (5). To justify this we need to introduce a small amount of dissipation into the system. The degree of mode localization is insensitive to the dissipation provided the dissipation length scale is greater than the localization length scale. Thus to evaluate the localization scale we may consider quite large dissipation, such that the dissipation scale is much less than the length of the chain. One can then use outgoing boundary conditions as above. In this regime dissipation can affect the response by a multiplicative factor but the shape of the response remains unaltered, so that it does not matter that in the real structure on which the measurements are made the dissipation scale is actually longer than the length of the chain.

For frequencies within the passband, the diagonal element $(R_0)_{kk}$ is pure imaginary since q is real, and so the term linear in the fluctuation K in Eq. (24) gives no contribution to the localization. The lowest order effect comes from the next term, so that in the passband, for small disorder, the amplitude decay constant is given approximately by

$$\alpha = \text{Re } \gamma \approx [2N(2V \sin q)^2]^{-1} \times \text{Re} \left(\sum_{k,j} K_k K_j \exp(2iq|k - j|) \right). \quad (26)$$

Noting that

$$\text{Re} \{ \exp(2iq|k - j|) \} = \text{Re} \{ \exp[2iq(k - j)] \},$$

this equation becomes

$$\alpha \approx \frac{1}{2N} \left| (2V \sin q)^{-1} \sum_j K_j \exp(2iqj) \right|^2; \quad (27)$$

in other words, the localization scale is proportional to the Fourier transform of the disorder in pendulum frequencies. Finally, for typical distributions of ω_k the deviations from the mean are uncorrelated from pendulum to pendulum, so terms in Eq. (26) with $k \neq j$ vanish and one has

$$\alpha \approx \frac{1}{2} \langle K_j^2 \rangle / (2V \sin q)^2. \quad (28)$$

The amplitude decay constant (one-half the intensity decay constant) is proportional to the mean-square fluctuation $\langle K_j^2 \rangle$ and therefore to the square of the distribution width W . For the statistical distribution defined at the beginning of this section.

$$\langle K_j^2 \rangle = W^2/3. \quad (29)$$

These results show that as the disorder tends to zero the localization range in one dimension tends to infinity, but that all the modes remain localized when one looks on a sufficiently large scale. We have shown this by considering the propagation from end to end of a finite chain. The same results would hold true for propagation between two points N steps apart on an infinite chain, provided N is much larger than the localization length. Think, for example, of coupling segments of length N together to form the infinite chain. The interaction between modes on adjacent segments, which depends on the modal amplitudes on the end pendula, becomes exponentially small for large N . Thus the coupling is much less than the frequency difference between the modes. The modes on adjacent segments are therefore effectively uncoupled and independent.

C. Formula for localization on the string

The results of Secs. IIA and B may be adapted to the experiments with masses on a vibrating string by means of the discussion in Sec. I. The pendulum frequencies ω_k are given by Eq. (12). In the experiments variations in mass spacings are of the order of 2% so in this equation $\epsilon_k \approx 0.02$. By expanding to first order in ϵ_k one obtains the variation in pendulum frequencies and to this order Eq. (23) gives the fluctuating part of the matrix M as

$$K_k = \omega_k^2 - \Omega^2 \approx 2\Omega^2 \epsilon_k, \quad (30)$$

where $\Omega = n\pi(t/\rho)^{1/2}$.

In the experiments we are mainly in a situation of weak disorder, $W/V < 1$. If the mass spacing is uncorrelated down the chain, Eq. (30) may be substituted directly into Eq. (28) to obtain the decay constant α . If on the other hand it is the mass displacements which are uncorrelated one obtains a simpler result in which the localization α is independent of q , i.e., of the frequency within the passband. When Eq. (27) is expanded by setting $\epsilon_j = \xi_{j+1} - \xi_j$ a factor of $\sin^2 q$ cancels out leaving

$$\alpha \approx \frac{2}{N} \left(\frac{\Omega^2}{V} \right)^2 \left| \sum_j \exp(2iqj) \xi_j \right|^2 = 2 \left(\frac{\Omega^2}{V} \right)^2 \langle \xi_j^2 \rangle, \quad (31)$$

where ξ_j is the displacement of mass j divided by the mean mass spacing. This result is more convenient for comparing

with the experiment since the measurements give an average of α through the band. We therefore aimed to make the mass displacements rather than the spacings uncorrelated down the chain, in so far as any difference can be discerned for such a short chain.

Although the experiments are designed to focus attention on the weak disorder limit, even a spacing variation as small as 2% can lead to values of the disorder-to-coupling ratio W/V of order unity for the equivalent pendulum model of the string. Such values occur in the higher passbands as is pointed out in Sec. III. To allow for this, experiments are compared to an approximate formula for α which interpolates between the strong and weak disorder limits. This formula is

$$\alpha = \frac{1}{2} \ln [1 + 4(\Omega^2/V)^2 \langle \xi_j^2 \rangle]. \quad (32)$$

For small disorder expanding the logarithm reproduces Eq. (31). For large disorder the argument of the logarithm is of order $(W/V)^2$ from Eqs. (30) and (29), and so the formula reproduces Eq. (22) to leading order in W/V , i.e. without constants of order unity.

It may be pointed out here that a cross check on the degree of disorder in the pendulum model of the string can be obtained from the band broadening observed in the irregular system. Matrix algebra methods¹³ yield the relation

$$\langle (\Omega_j^2 - \Omega^2 - 2V)^2 \rangle = 2V^2 + \langle K_j^2 \rangle,$$

where Ω_j are the normal mode frequencies of a chain of coupled pendula and the average on the left-hand side is taken over the passband. Thus the increase in passband width as determined from the second moment of the band about its mean Ω provides a direct measure of the disorder.

III. THE MEASUREMENTS

The apparatus consisted of a length of thin high-tensile steel wire stretched between two supports mounted on an optical bench. The supports were as massive as could be achieved easily, to minimize coupling between the string and the bench. The string was tensioned close to its breaking strain, so that it behaved as nearly as possible like an ideal flexible string: that is the contribution of bending stiffness to any forces was minimized. (Even so, as we shall discuss, effects of finite bending stiffness are seen in the measurements.) The length of the string between the supports was 800 mm. Seven small lead weights (the smallest size of fishing line weight) were attached to the string, initially dividing it into eight equal lengths of 100 mm. The weights were secured with cyanoacrylate adhesive. For the second phase of the experiment, the masses were moved slightly to give a controlled amount of irregularity to the system. The positions of the masses then were 98, 203, 301, 398, 499, 602, and 704 mm from one end. In other words, the deviations from regular positions varied by about 2% of the regular spacing.

In all the experiments, the string was excited by plucking gently with a loop of 47 SWG copper wire: by pulling such a loop of wire until it breaks, it is possible to impart a step function force with rather accurately repeatable amplitude. The string motion was observed by means of a horse-shoe magnet with suitably shaped pole pieces placed athwart

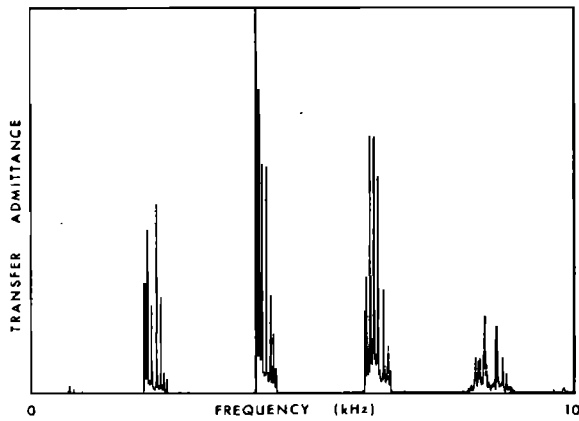


FIG. 3. Transfer admittance between points 15 mm from the two ends of the string, with regularly spaced masses. The curve represents the modulus of the admittance, plotted on a linear vertical scale and autoscaled to fit the box. The frequency scale is linear, from 0–10 kHz.

the string at the point of observation. This gives an induced voltage across the ends of the string which is proportional to the velocity at the observed point. This voltage was digitized, after an appropriate impedance-matching preamplifier, by a 12 bit analog-to-digital converter into the memory of a CA LSI4/30 minicomputer. The driving-point measurements were digitized at 20 kHz, and the transmission measurements were digitized at 40 kHz.

Since the aim throughout these measurements was to obtain accurate estimates of the driving-point and transfer admittances of the string at various points, we did not want to have any problems with windowing resulting from the fact that the reverberation time of the string was invariably much longer than the storage capacity and FFT capacity of the machine. To avoid any such difficulties, the trick of circular logging was used, which we now explain. Suppose the true time response whose Fourier transform we want is $f(t)$, with Fourier transform $F(\omega)$. We have sampled values of $f(t)$ at times $n\Delta$, and we wish to obtain the best estimate of $F(\omega)$ using an FFT whose maximum length N is limited by the machine size. Note now the Poisson summation formula

$$\sum_n f(t - nT) = \left(\frac{2\pi}{T}\right) \sum_n F\left(\frac{2\pi n}{T}\right) e^{2\pi i n t / T}, \quad (33)$$

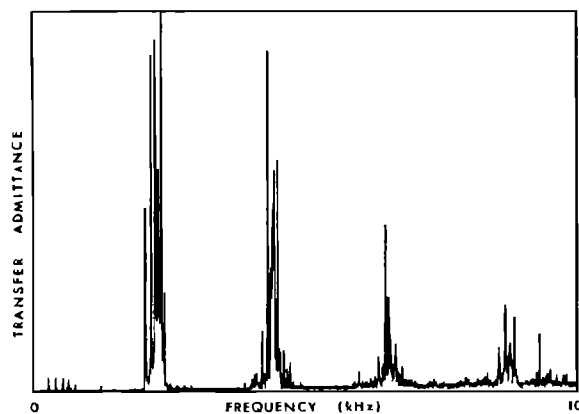


FIG. 4. Transfer admittance between points 15 mm from the two ends of the string, with irregularly spaced masses. All details as for Fig. 3; again, the graph is autoscaled so that the vertical scales are different in the two cases.

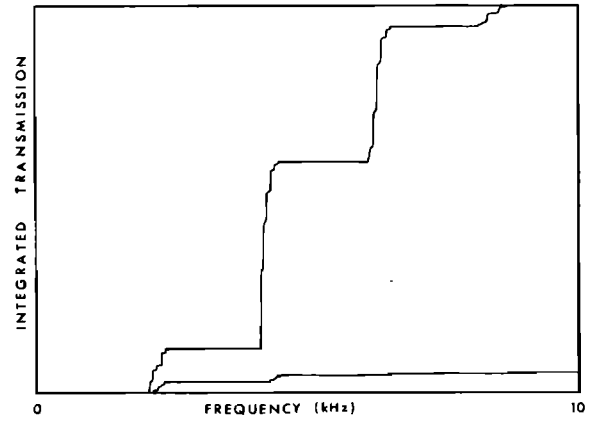


FIG. 5. The curves show the integrated square of the curves in Figs. 3 and 4. The upper curve shows the regular case, and the lower curve the irregular case. The frequency scale is again linear, 0–10 kHz.

where $T = N\Delta$. The right-hand side of Eq. (33) is the discrete Fourier transform which we wish to calculate, so Eq. (33) tells us that we should take the FFT not of $f(t)$ alone, but of $\sum f(t - nT)$, which is $f(t)$ turned into a periodic function with period T by adding in all values of f delayed by multiples of that interval. In other words, we take our buffer in the

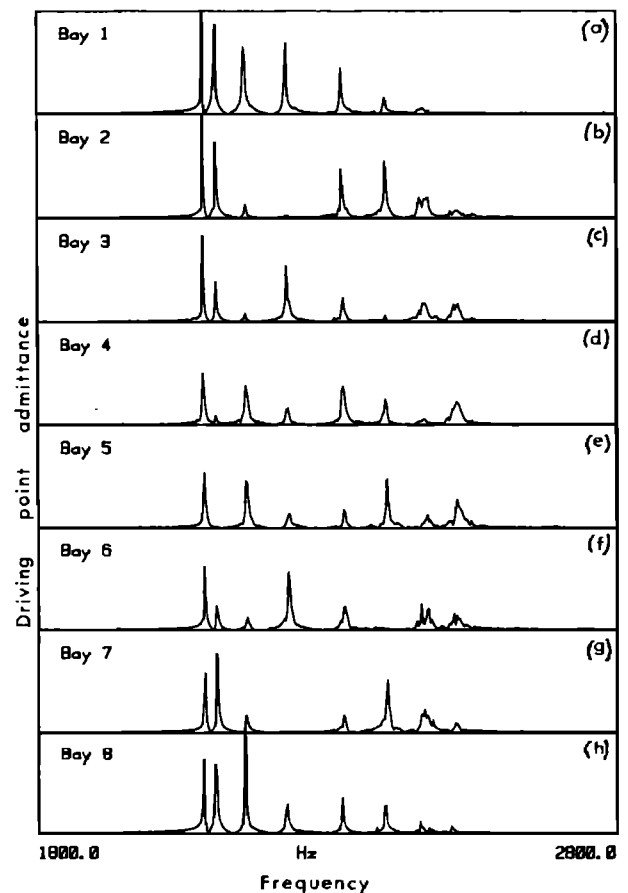


FIG. 6. (a)–(h) The modulus of the driving point admittance at the center of each of the eight bays, with the masses spaced regularly. Both scales are linear. The frequency range covers the second passband of the string. Notice that as any one mode is followed through the eight bays, it has significant amplitude in most of them: the modes are extended throughout the structure. Put a different way, in any one bay it can be seen that there are eight separate peaks in the spectrum since each mode appears in each bay.

computer memory (chosen to have length a power of 2 for later FFT convenience) and digitize the string response into that buffer treating it as circular and adding the new digitized value to the previous total. We then sample in this circular manner for a sufficiently long time to contain all the essentially nonzero portion of the (decaying) pluck response of the string. When we then FFT this time series we obtain a good estimate of the Fourier transform of the continuous time function which has been digitized, with no problems of windowing, sidebands, etc.

In fact in the measurements taken here, an additional step was performed between digitizing and FFT. Since we have digitized the step response of the string and we really want the Fourier transform of the impulse response, the time series was differentiated. This operation has to be treated with some care, because of the tendency of a relatively low-frequency signal to be swamped by high-frequency noise in the process. To control this problem, a differentiation algorithm is needed which has a frequency response which is close to $i\omega$ throughout the frequency range of interest but

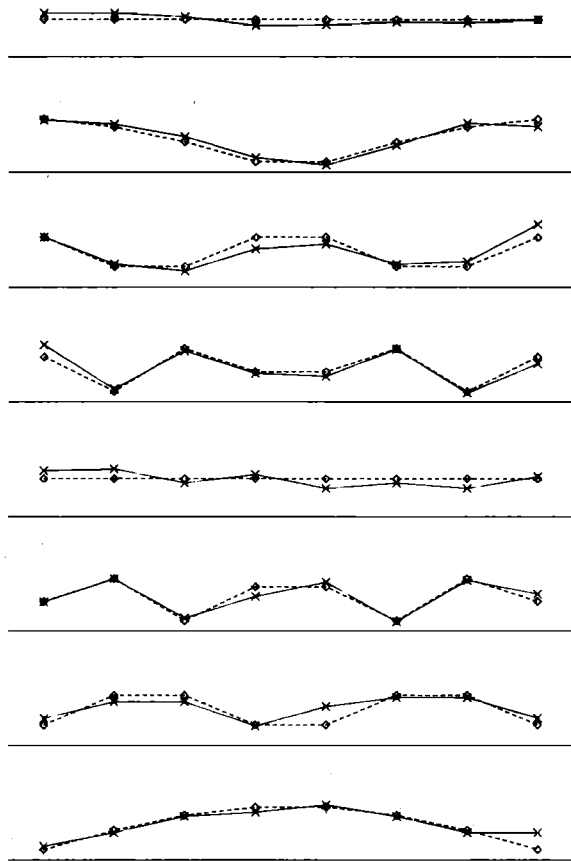


FIG. 7. Rectified mode shapes deduced from the graphs of Fig. 6, by measuring peak heights and taking their square roots (shown as crosses connected by lines). These are compared with the theoretical shapes for a periodic system (shown as diamonds connected by dashed lines) given by the rectified versions of the motions at the center of each bay in Fig. 2(a). Each mode is normalized so that the sum of squares of the eight points is constant: the experimental modes taken directly from the graphs have slightly differing amplitudes because of variations in damping factor, and this is irrelevant to the comparison of shape between localized and extended which we wish to make. The modes are arranged in order of frequency with the lowest frequency at the top.

which rolls off at higher frequencies. The method used involved fitting a least-squares cubic to five data points at a time, and using the derivative of that cubic as our estimate of the derivative of the original time series. This method performed very satisfactorily with the rather clean signals obtained from these string observations.

Having followed these steps for any given take in the series of measurements, we have the complex admittance of the string in the computer. In all cases, an FFT size of 8192 was used. However, a single observation is not really sufficiently reliable for the purpose in hand, since we require accurate estimates of relative peak heights in the various spectra. Thus for each measurement five takes were made, and the complex spectra linearly averaged. This gives both a better final answer in the average, and an idea of the spread among successive repeats of the same measurement which is important for accuracy assessment.

We are now ready to describe the detailed measurements made. These were of two kinds. First, transmission from end to end of the string was measured in the regular and irregular configurations. This was done by plucking at 15 mm from one end of the string and observing at the same distance from the other end. These results are shown in Figs. 3 and 4. In each case, linear spectral amplitude is plotted against frequency on a linear scale from 0–10 kHz. The

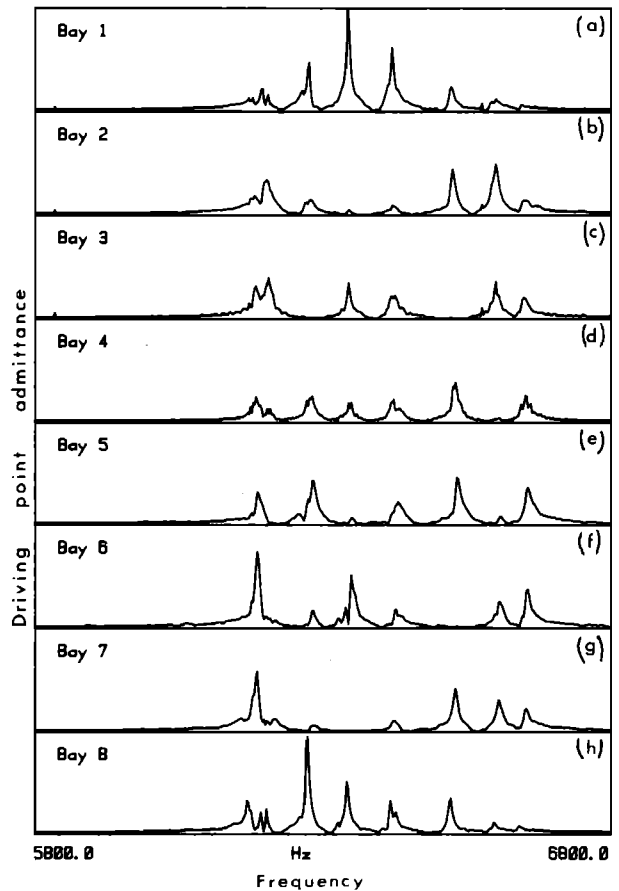


FIG. 8. (a)–(h) Driving point admittances at the center of each bay just as in Fig. 6, but over a frequency range covering the fourth passband of the string. The modes here are still extended, still agreeing quite well with periodic theory.

structure of pass and stop bands is clearly visible in both cases. The very low-frequency modes illustrated in Fig. 2(b) are barely visible since not much energy is put into them. The next four passbands are clearly visible.

In Fig. 5 are shown two monotonically climbing curves, which are the integrated square of the amplitudes in Figs. 3 and 4. These curves enable us to decide easily how much energy is transmitted by the set of modes in each passband: we simply measure the heights of the "steps" which the curves describe as they pass through each band. A large difference in total transmitted energy between the regular and irregular cases is immediately visible and it is clear that the attenuation gets greater as we go to higher passbands. This will be discussed further and compared with the theoretical predictions in the next section.

The second type of measurement made was of driving-point admittance of the string at the center of each bay in turn. The object of this was to determine the mode shapes within some of the passbands, to see the mode localization behavior directly. This was done by making use of Eq. (1) with $x = x'$. This tells us that the peak height of a given mode as a function of position x is the square of the mode amplitude as a function of x . Thus by measuring the peak heights of each of the eight modes in a band in each bay in turn, we can calculate the square root of these heights and deduce mode amplitudes except for sign. In practice there is little

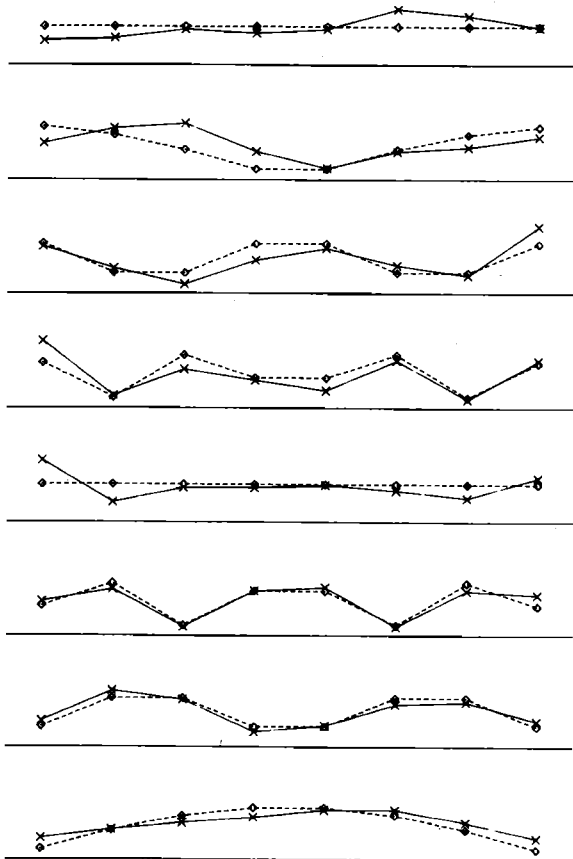


FIG. 9. Rectified mode shapes for the fourth passband on the string with regularly spaced masses (crosses) compared with the theoretical predictions for the precisely regular system as in Fig. 7 (diamonds).

difficulty seeing what sign is appropriate at least in the regular case, given the theoretical expectations shown in Fig. 2(a).

These driving-point measurements were made at the center of each bay, so that we were able to study in detail the modes of the second and fourth passbands [$n = 1$ and 3 in Eq. (6)]. The modes of the third and fifth bands have of course nodes in this position and are thus not observed. Figure 6(a)–(h) shows the spectra in the frequency range of the second passband for the regular configuration. Figure 7 then shows mode shapes for that band deduced from the peak heights in Fig. 6. These are compared with rectified versions of the theoretical mode shapes of Fig. 2. Figures 8(a)–(h) and 9 give the same information about the regularly configured string in the frequency range of the fourth passband. Figures 10 (a)–(h) and 11 give the spectra and mode shapes for the second passband in the irregular case.

Figure 12 (a)–(h) shows the spectra for the fourth band in the irregular case. Since in this case the modes are very strongly localized, it is hard to see that there are still eight modes in the band in this case from the eight separate spectra. However careful inspection of Fig. 12 with the aid of a straight edge confirms that there are. Figure 13 shows the mode shapes for this band. Note that the noise level in modal amplitudes in Fig. 12 is greater than in the other three cases,

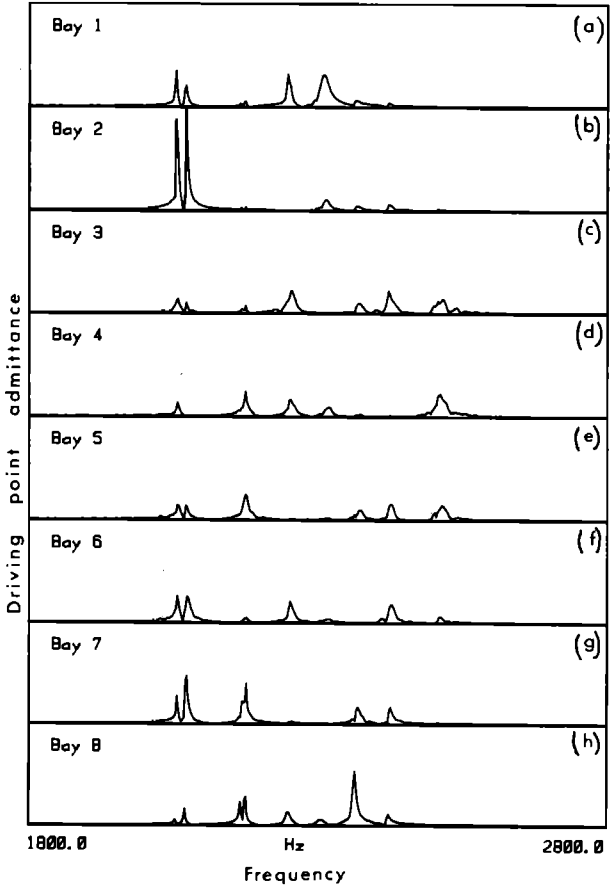


FIG. 10. (a)–(h) Driving point admittances at the center of each bay just as in Fig. 6, but with the masses moved slightly to their irregular positions. The frequency range covers the second passband of the string. The modes here are still quite extended, but agreement with periodic theory has lessened as expected.

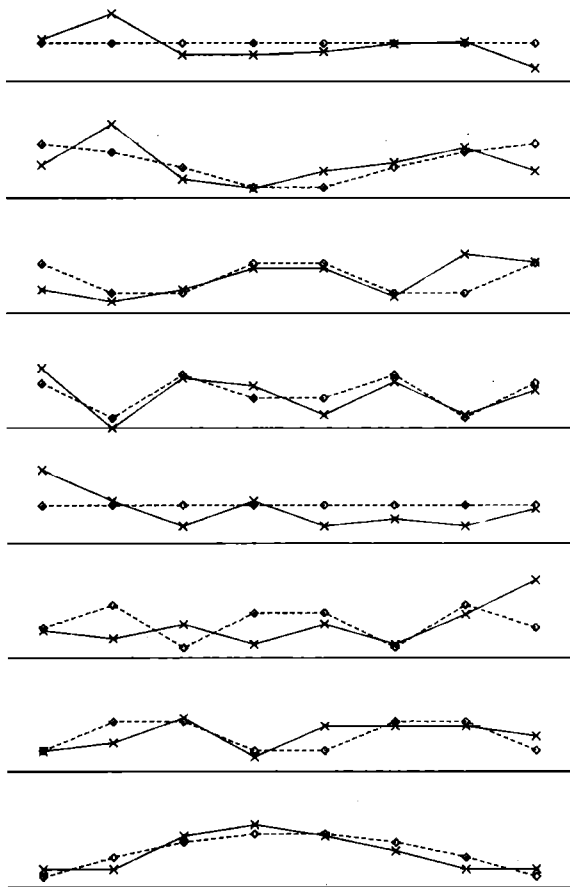


FIG. 11. Rectified mode shapes for the second passband on the string with irregularly spaced masses (crosses) compared with the theoretical predictions for the precisely regular system as in Fig. 7 (diamonds).

since with the much more strongly localized modes it is hard to measure accurately the peak heights away from the bays in which the mode in question is strong.

IV. DISCUSSION OF THE RESULTS

We can now compare these results with the theoretical predictions of the magnitude of the localization effect given in Sec. II. Before proceeding to such a detailed comparison, however, it is worth observing the very clear qualitative agreement of the observations with the theory. The difference between the modes in Figs. 6 and 7, which agree well with periodic theory, and those of Figs. 12 and 13, where localization is strong, is very striking. This produces the greatly reduced energy transmission in the irregular case, especially in the higher passbands, revealed by the two curves in Fig. 5.

To make quantitative comparisons with theory, we first need to know the strength of the coupling between bays on our particular string. As explained in Sec. I, this is most easily done by measuring the width of each passband compared with the spacing between bands, in the regular configuration. Table I shows the mode frequencies (with a resolution of some 3 Hz) for the second and fourth passbands in both the regular and irregular cases. Now from Eq. (5) and the following discussion, we can deduce that the ratio Ω^2/V

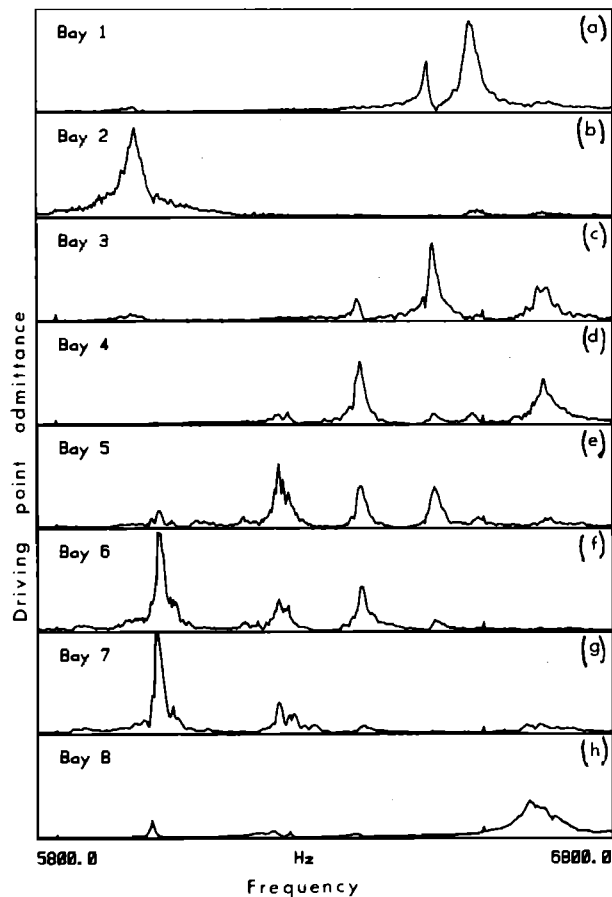


FIG. 12. (a)–(h) Driving point admittances at the center of each bay just as in Fig. 8, with the masses moved slightly to their irregular positions. The frequency range covers the fourth passband of the string. Now the modes are strongly localized. Observe that in any one bay, it is far from apparent that there are eight peaks in the band. Only when all eight bays are superimposed can the eight peaks be counted with any reliability.

which enters Eq. (32) has the approximate value 8.6 for the second band, and 25.5 for the fourth band.

From these values of the coupling parameter and the known amount of randomness in the irregular configuration, we can now obtain a cross check on the theory. The irregularity results in the bands being broadened in the irregular case, and we can predict the order of magnitude of that broadening as explained at the end of Sec. IIC. This we can compare with the actual band broadening revealed in the third and fourth columns of Table I. This comparison confirms the general appropriateness of the theory, and tells us that in the irregular case, the coupling-to-disorder ratio V/W is large for the second passband (weak disorder, small band broadening) and of order unity for the fourth band (quite strong disorder, band broadening of the order of the bandwidth).

One other observation we can make from Table I is that the widths of the bands in the regular case are not behaving quite as an ideal textbook string model would lead us to expect. That model would suggest that the bands should get narrower in proportion to $1/n$ as the bandnumber n increases. However it is apparent that the fourth band is much the same width as the second. Further measurements, including other bands, show that in fact the width decreases

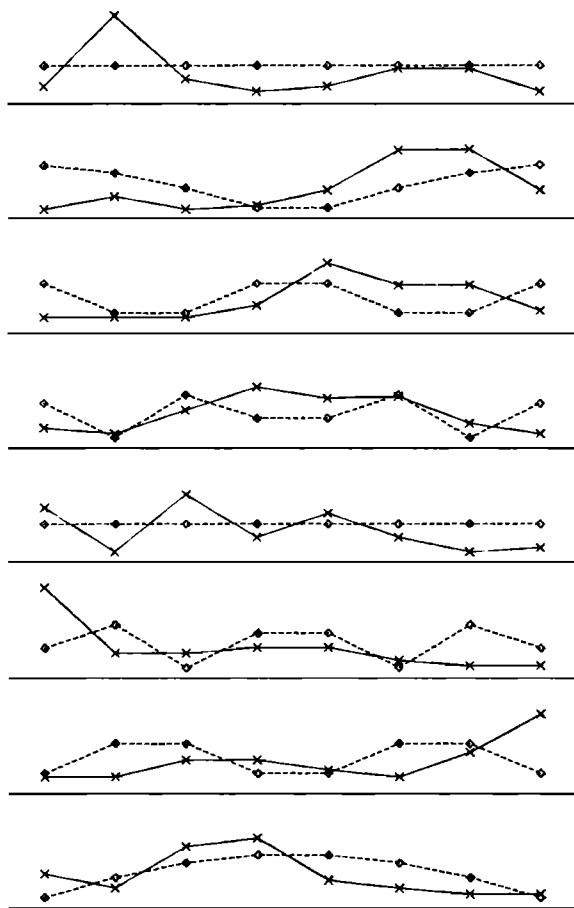


FIG 13. Rectified mode shapes for the fourth passband on the string with irregularly spaced masses (crosses) compared with the theoretical predictions for the precisely regular system as in Fig. 7 (diamonds).

from the second to the third band, but then increases steadily. We believe this effect is caused by nonvanishing bending stiffness in the string. Bending stiffness can have such a noticeable effect at such low frequencies because near the masses, the string is bent at a very small radius of curvature [as shown in Fig. 2(a)], much smaller than would occur at that frequency on a string with no masses. The coupling of adjacent bays through the masses is strengthened by the effect of nearfield bending components, thus broadening the

TABLE I. Mode frequencies in Hz for the second and fourth passbands with regular and irregular mass spacing. The mean frequency of both bands has slipped down a little between the regular and irregular cases: this is a result of a small temperature variation beyond our control changing the tuning of the string, and does not affect the conclusions of this article at all.

Regular		Irregular	
Band 2	Band 4	Band 2	Band 4
2085	6180	2052	5965
2107	6202	2070	6008
2157	6272	2172	6223
2230	6342	2247	6365
2325	6417	2310	6494
2400	6520	2370	6561
2467	6600	2422	6654
2522	6647	2515	6684

passbands. Estimates of the expected magnitude of the effect are easy to make, and confirm that it is consistent with the observations.

We are now ready to compare the energy attenuation by disorder with the predictions. By measuring the heights of the steps between bands on the two curves of Fig. 5, we deduce that the energy reaching the final bay in the disordered case divided by the same thing in the regular case is 0.25 for the second band, 0.032 for the third band, and 0.011 for the fourth band. (It should be pointed out these measurements were made on a much larger-scale copy of the picture than that reproduced here, to give the required accuracy.) These are to be compared with the prediction of Eq. (32) above. The appropriate value of the disorder measure $\langle \xi_j^2 \rangle$ is $(0.024)^2$. From the values of Ω^2/V given above, we can deduce values for α of 0.08 for the second band, and 0.45 for the fourth band. Less accurate measurements of Ω^2/V from the bandwidth in Fig. 3 suggest a value around 0.3 for the third band. Now the energy attenuation ratio between disordered and regular configurations is given by $(e^{-7\alpha})^2$, so our predictions of this are 0.33 for the second band, 0.01 for the third band, and 0.0017 for the fourth band. Thus band 2 agrees to reasonable accuracy, and band 4 is out by a factor 6.

A factor 6 in error sounds like a lot, but bear in mind that we are dealing with exponential decays, where a small error in the exponent produces a rapidly growing error in attenuation. In fact the agreement between theory and experiment is to within 20% in the exponent for bands 2 and 3 and 40% for band 4. These discrepancies are entirely consistent with the order of accuracy expected from the predictions with such a short structure. The predictions are after all ensemble averages over different randomized structures, and with only eight bays in our structure, the statistical fluctuations in that average are large. (We intend to discuss in detail this question of ensemble averaging and the sources and magnitudes of various kinds of expected deviations from the predictions in a future article.) Thus we conclude that the measurements presented here are consistent with the theory.

One question that might be asked about the measurements, since such strong attenuation is produced by 2.4% irregularity, is how much attenuation was present in the supposedly regular case as a result of inevitable errors in positioning the masses. The accuracy in positioning the masses is about 0.5 mm. Feeding this value for irregularity into Eq. (32) yields energy attenuations of 0.95 for the second band, and 0.63 for the fourth band. Thus the attenuation due to accidental irregularity was at most about one half, whereas with the 2.4% irregularity, only 1% of the energy got through to the eighth bay in the same band. This gives an idea of how strong the effect of localization can be once it begins to be significant, and puts in perspective the deviation of the measurement from the prediction.

V. CONCLUSIONS

Measurements on a stretched string divided into eight bays by point masses have been made, and checked against theoretical predictions of the effect of irregularity in the mass spacings. Observations were made of energy transmis-

sion from end to end of the string, both in a periodic configuration and in a slightly disordered configuration. Levels of energy attenuation in the disordered case were observed which are consistent with the theoretical estimates. These levels of attenuation were in some cases quite large: with only 2.4% standard deviation in the mass positions, in the fourth passband it was some 99%. One is forced to conclude that such attenuation effects due to Anderson localization might sometimes be of considerable significance in structural vibration problems. The mode shapes in the second and fourth passbands were also measured, and these show very clearly the origin of the energy attenuation in localization of the normal modes.

It should be noted that, as previously described,¹ the strength of Anderson localization for a given disorder level depends on the dimensionality of the system. In one dimension, as is the case for the system studied here, it is known that all modes are localized for arbitrarily small disorder. This is still believed to be true in two dimensions, but the localization scale is far longer for a given level of disorder. In three dimensions, a finite threshold of disorder must be passed before all modes become localized. It is interesting to note that in solid-state physics, the main interest is quite naturally in three-dimensional systems. The one-dimensional case is regarded primarily as a theoretical curiosity, studied only because it is analytically far simpler. In acoustics by contrast, we are frequently interested in systems in which the near periodicity is indeed one-dimensional—strutted plates or railway lines for example. Thus we are in the fortunate position of being able to make practical use of the simplest case of the behavior, while those who have done most work on the phenomenon have to contend with the harder cases.

ACKNOWLEDGMENT

This work has been carried out with the support of the Procurement Executive, Ministry of Defence.

APPENDIX: EXPANSION OF THE LOGARITHM OF A DETERMINANT

In this Appendix we show how to expand the quantity

$$\Gamma(z) = \ln[\det(zI - M)], \quad (\text{A1})$$

which appears in Eq. (17) with z set equal to ω^2 . By using Eq. (18) as an intermediate step, one can also write

$$\Gamma(z) = \text{tr}[\ln(zI - M)]. \quad (\text{A2})$$

We wish to expand Eq. (A2) in powers of M_p , where $M = M_0 + M_p$, and M_0 and M_p do not necessarily commute. The expansion of a function of two noncommuting matrices A and B is in general very complex and involves commutators (A, B) . There is, however, a nontrivial exception to this rule in the inverse of $A - B$ which has the expansion

$$(A - B)^{-1} = A^{-1} + A^{-1}BA^{-1} + A^{-1}BA^{-1}BA^{-1} + \dots \quad (\text{A3})$$

Now set $A = zI - M_0$ and $B = M_p$ so that the derivative of Eq. (A2) expands to

$$\frac{\partial}{\partial z} \ln(zI - M) = (zI - M)^{-1} = R_0(z) + R_0(z)M_p R_0(z) + \dots, \quad (\text{A4})$$

where

$$R_0(z) = (zI - M_0)^{-1}.$$

The trace of the above equation may be integrated by means of the identities

$$\frac{\partial}{\partial z} R_0(z) = -R_0(z)^2$$

and

$$\text{tr}\left(\frac{\partial}{\partial z} [R_0(z)M_p]^n\right) = -\text{tr}\{n[R_0(z)M_p]^{n-1}R_0(z)\}, \quad (\text{A5})$$

which depends on the invariance of the trace of a product under cyclic permutations of the constituent factors. Therefore one has

$$\begin{aligned} \Gamma(z) &= \text{tr}[\ln(zI - M)] \\ &= \text{tr}[\ln(R_0)] - \text{tr}\left(\sum_{n=1}^{\infty} \frac{1}{n} (R_0 M_p)^n\right). \end{aligned} \quad (\text{A6})$$

Substituting this in Eq. (17) gives the expression Eq. (20). Note that Eq. (A4) cannot be integrated without first taking the trace. There is correspondingly no simple expansion of $\ln(A - B)$ without introducing commutators.

¹C. H. Hodges, "Confinement of vibration by structural irregularity," *J. Sound Vib.* **82**, 411-424 (1982).

²V. V. Glushkov and M. N. Kuz'michev, "Transmission of flexural waves across a system of parallel beams," *Sov. Phys. Acoust.* **26**, 206-208 (1980).

³A. S. Bansal, "Free-wave propagation through combinations of periodic and disordered systems," *J. Acoust. Soc. Am.* **67**, 377-389 (1980).

⁴Alan R. Wenzel, "Radiation and attenuation of waves in a random medium," *J. Acoust. Soc. Am.* **71**, 26-35 (1982).

⁵J. M. Ziman, *Principles of the Theory of Solids* (Cambridge U. P., Cambridge, 1964), p. 31.

⁶P. W. Anderson, "Absence of diffusion in certain random lattices," *Phys. Rev.* **109**, 1492-1505 (1958).

⁷N. F. Mott and P. W. Anderson, "Nobel Lectures in Physics for 1977," *Rev. Mod. Phys.* **50**, 191-208 (1978).

⁸Lord Rayleigh, *The Theory of Sound* (Macmillan, London, 1894 and Dover, New York, 1945).

⁹D. C. Herbert and R. Jones, "Localized states in disordered systems," *J. Phys. C: Solid State Phys.* **4**, 1145-1161 (1971).

¹⁰D. Thouless, "Localization distance and mean free path in one-dimensional disordered systems," *J. Phys. C: Solid State Phys.* **6**, L49-L51 (1973).

¹¹R. Courant and D. Hilbert, *Methods of Mathematical Physics* (Interscience, New York, 1953), Vol. 1.

¹²This result is implicitly assumed but seldom stated in much of the solid state work. The approach of Ref. 11 could probably be adapted to provide a formal proof.

¹³J. M. Ziman, *Models of Disorder* (Cambridge U. P., Cambridge, 1979), pp. 348, 349.